



**LOADING NOISE PREDICTION USING EXPERIMENTAL DATA  
FROM HELINOISE TEST CAMPAIGN AT DNW**

**BY**

**S. IANNIELLO**

**CIRA, ITALIAN AEROSPACE RESEARCH CENTER  
CAPUA, ITALY**

**TWENTIETH EUROPEAN ROTORCRAFT FORUM  
OCTOBER 4 - 7, 1994 AMSTERDAM**

# LOADING NOISE PREDICTION USING EXPERIMENTAL DATA FROM HELINOISE TEST CAMPAIGN AT DNW

S. Ianniello

*C.I.R.A.*,

*Italian Aerospace Research Center*

*Capua, Italy*

## Abstract

Exploiting the aerodynamic and acoustic data-base provided by HELINOISE experimental program, numerical prediction of rotor noise signatures is performed for different flight conditions. The data-fitting problem for blade airload reconstruction is addressed and solved with different interpolating models. The comparisons between experimental and numerical results are presented in time domain, through the acoustic pressure time histories visualization.

$p'$	acoustic pressure
$\tilde{p}$	blade pressure
$c_0$	speed of sound in the undisturbed medium
$\rho_0$	air-density in the undisturbed medium
$\vec{n}$	unit vector normal to the blade surface
$\vec{r}$	$= \vec{r}/r$ , unit vector in the radiation direction
$r$	$=  \vec{r}  =  \vec{x} - \vec{y} $ , distance between source and observer
$\theta$	angle between $\vec{r}$ and $\vec{n}$
$M$	Mach number $=  \vec{M}  =  \vec{v} /c_0$
$M_n$	$= \vec{M} \cdot \vec{n}$
$M_r$	$= \vec{M} \cdot \vec{r}$

## 1. Introduction

Over the last few years, much research effort in the helicopter aeroacoustics has been devoted to the evaluation of quadrupole noise; the physical phenomena related to this important component of sound field make it a very challenging subject for aeroacousticians. From a theoretical point of view, no particularly interesting aspect arise from the other two components, which contribute to the determination of acoustic pressure field generated by the rotor blade. The *thickness noise* term is only related to body shape and motion: its contribution is very significant only for observer positions in the rotor plane and strongly increases with the rotational speed. The prediction of thickness noise is very simple when the numerical tool is able to give a complete description of body shape and motion. Instead, the *loading noise* term

is related to the aerodynamic pressure on the surface: its contribution is determinant for subsonic tip blades and observer locations out from the rotor plane. The numerical evaluation of this component gives no problem when an accurate knowledge of pressure distribution on the blade surface is available. But, in this context, what is the meaning of word *accurate*? The aerodynamic data may come from numerical codes (with all approximations related to the adopted model) or, alternatively, from experimental tests; in the latter case the airload distribution must be built from the knowledge of a few points upon the body, where the pressure transducers are placed. Thus the usefulness of very expensive tests (often conducted just for the validation of numerical tools) is not so immediate and it is not clear neither what kind of fitting procedures has to be adopted, nor how it will affect the predicted acoustic signatures. These questions are often disregarded in the acoustic literature, but the *reliability* of a numerical code highly depends on the answer given to them.

Aim of this paper is to address the above problem, through the use of a special version of HERNOP code [1] and the large data-base obtained during the Brite/Euram project *HELINOISE*, where a very extensive test-campaign was conducted in the DNW wind tunnel [2], for a four-bladed helicopter rotor at different flight conditions. Exploiting the modular structure of the computational tool two different codes are extracted: one performs the acoustic calculations and the other one extrapolates the airload distributions from experimental data, following different interpolating models. Experimental signatures are then compared with the acoustic pressure time histories calculated through integral formulations.

## 2. HELINOISE test-campaign

During the *HELINOISE* project an extensive experimental program was launched, employing a 40% geometrically and dynamically scaled highly instrumented main rotor model of BO-105 helicopter placed in a high quality aeroacoustic wind tunnel. The generation of a large airload and acoustic data base was the main object of the experimental effort; such extensive and fundamental data, crucial in validating aerodynamic and aeroacoustics codes, was not yet available within the European helicopter noise research community. These data are just suitable for our purposes, since many cases refer to subsonic tip blades with a microphone always positioned below the rotor plane, where the loading noise signature is predominant.

Altogether 124 pressure transducers have been placed upon the body, mainly distributed along three different sections close to blade tip (at  $0.75$ ,  $0.87$  and  $0.97r/R$ ), and spanwise near the leading edge, to guarantee an high spatial resolution of blade pressure. The rotor has a diameter of 4 m with a root cut-out of 0.350 m and a chord length of 0.121 m; a NACA 23012 airfoil was uniformly distributed spanwise, with a  $-8^\circ$  of linear twist (Fig. 1). The pressure sensors were submerged in the blade surface layer being in contact with the surface pressure field via small dimensions, very short tubes (the sensors effective measuring area corresponded to a circle of 0.5 mm diameter) to ensure the high spatial resolution for pressure field (the complete sensor characteristics are reported in reference [2]). The acoustic instrumentation consisted of linear inflow microphone array mounted on a ground based traverse system, with a maximum range of 11 m in flow direction; eleven microphones were arranged symmetrically with respect to the tunnel centerline and equally spaced 0.54 m apart. The array vertical position was usually 2.3 m below the rotor hub; the geometrical dimensions of the microphone array and its placement with respect to the rotor hub as well as the microphone spatial distribution are shown in Fig. 2a. The output signals of the 124 pressure transducers installed on one blade were pre-amplified by miniaturized amplifiers in the rotating frame and sampled at a rate of 2048/rev; raw data of 60 rotor revolutions were acquired and stored for subsequent calculation of ensemble averaged time histories and narrow band power spectra via FFT. A very time-efficient and sufficiently exact method was adopted to acquire acoustic data in the large plane below the rotor: the inflow microphone array was moved slowly (45 mm/s) and continuously

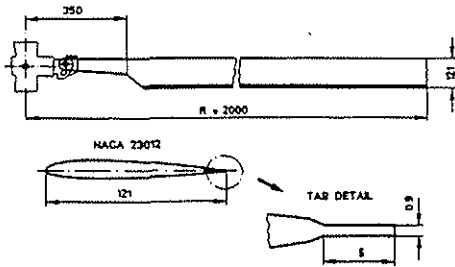


Figure 1 - Geometric characteristics of rotor blade.

over the measuring range of typically 4 to 5R (2R downstream and 2 to 3R upstream of the rotor center). The microphone signals were recorded continuously together with the streamwise microphone position and the synchronizing signals on analog tape. The acoustic data were acquired every half meter in streamwise direction providing typically 200 acoustic measurement points for each rotor condition; this acoustic grid is illustrated in Fig. 2b. At each pre-selected streamwise position the acoustic data acquisition system was started and the microphone signals were sampled at a rate of 2048/rev over a period of 30 rotor revolutions (1.7 seconds), giving a useful frequency range of 9 Hz.

### 3. Two codes for numerical simulation

The comparison between the experimental acoustic signatures and the corresponding numerical prediction has been performed with the HERNOP code, developed at C.I.R.A. during the *HELINOISE* project. Based on two well-known time domain Farassat formulations, the code performs loading noise calculation as the sum of different integrals on the body surface; the resulting signature is split up into far-field and near-field components. For our purposes, HERNOP has been divided into two different codes, named HENGEO (HELicopter Noise: GEOMETRIC module) and HENEXT (HELicopter Noise: EXperimental Test module).

HENGEO reads the aerodynamic input from a data base relating to the prescribed test-case; then it builds the blade (in the body frame of reference) and, on the grounds of the input grid and fixed stretching parameters, interpolates the experimental pressure values following different interpolating schemes. The presence of several pressure transducers at three different blade sections (which we call *fundamental chordwise stations*) suggests the use of a cubic-spline for the reconstruction of airload distribution; Fig. 3 shows the good fitting of data obtained for these values, for the hovering rotor test-case. Since from the acoustic point of view the most important region upon the blade is placed near the tip section (especially for high tip speed), the numerical grid is suitably built; thus, while in the original HERNOP version it is possible to increase the number of spanwise stations near blade tip by simply imposing a parabolic or cubic distribution for Y-coordinates, HENGEO fixes a region upon the blade (usually 50/60% from rotor hub) where just only three sections are placed. Then all the remaining spanwise stations are located in the outer blade region, where different stretching forms may also be adopted. On the other hand, the fundamental chordwise stations are all positioned in the *last* 25% of body surface, so it is possible (and very important) to determine an accurate pressure distribution just in that region. Two different HENGEO grids will be usually adopted in this paper, with different stretching models, to investigate about their influence on numerical calculations. Once we have moved upon the X-coordinates (chordwise) of HENGEO blade, it is necessary to choose a suitable form representing the spanwise pressure arrangement; thus, imposed the zero value at hub and tip sections, we may adopt a simple linear interpolation for all sections spanwise, or different mixed-schemes, using parabolic or cubic-spline partially distributed upon the surface. Still referring to hover test-case, Fig. 4 shows the complete pressure distributions (spanwise and 3D views) obtained through the use of fundamental chordwise stations only; here the spanwise interpolating scheme considers a cubic spline between 60% and tip section, with a parabolic decrease up to rotor hub. The *smoothness* of curve is obtained imposing the continuity of first derivative for interpolating forms in the

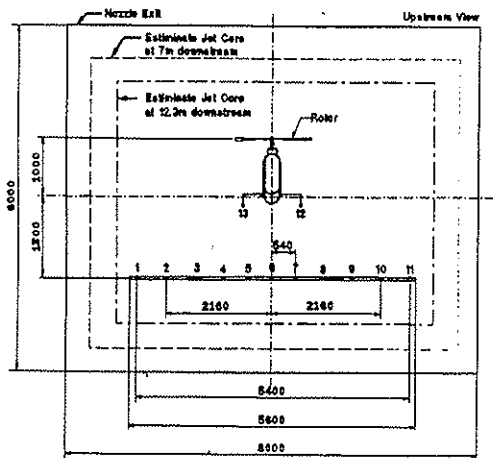


Figure 2a - Microphone array dimensions and microphone distribution.

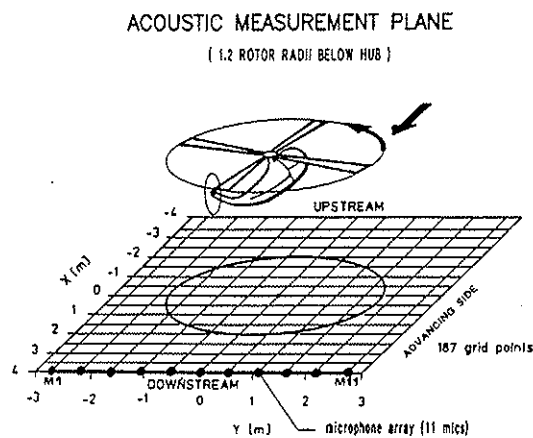


Figure 2b - Acoustic measuring plane.

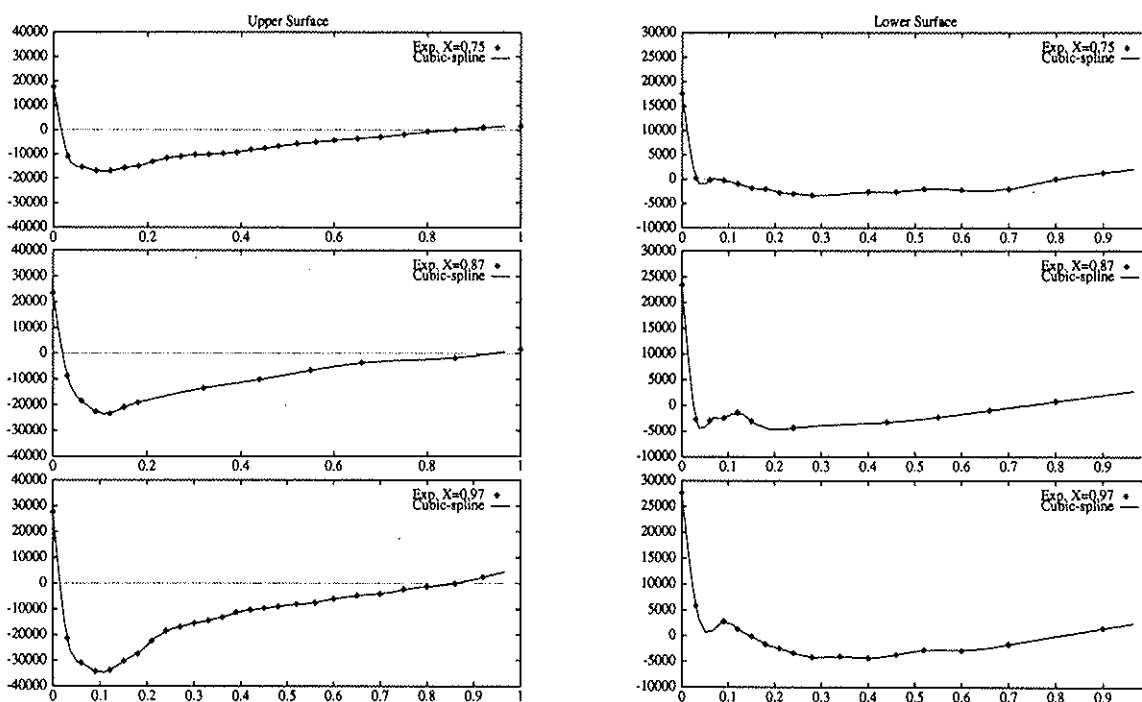


Figure 3 - This figure shows the good arrangement of cubic spline interpolation for aerodynamic input data upon the fundamental chordwise stations (upper and lower surface). The pressure values refer to the hovering rotor test-case.

connection point; the three dimensional views point out the good arrangement of calculated airload distribution. It is worthwhile to remember that this data manipulation has to be performed at each azimuthal position; this is true also for the hover test-case, where even though from a theoretical point of view just one blade airload is needed, the experimental data do not give a steady pressure value for all transducers.

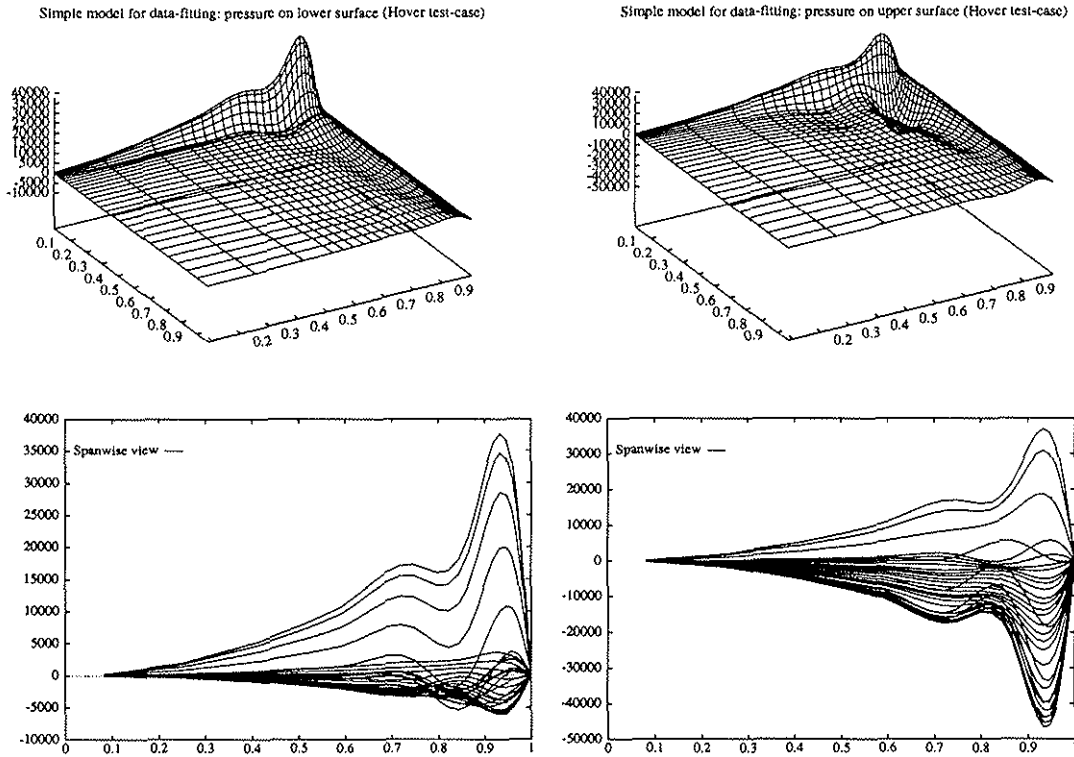


Figure 4 - The "simple model" builds the blade airload considering a parabolic pressure distribution between 0 and 60% of span and fitting the input data (in the last 40%) with a cubic spline.

Once HENGEO has performed its heavy interpolation work, the geometric grid and all calculated pressure distributions are stored into two output, unformatted files, to be read by HENEXT code. This computational tool, which may be considered the HERNOP *heart*, is based on Farassat time domain formulations 1 and 1A; knowing the body geometry and the aerodynamic data, it determines the emission time of each panel centroid and all retarded kinematic quantities appearing inside the integral kernels, evaluating thickness and loading noise through the equations:

$$4\pi p'_T(\mathbf{x}, t) = \frac{\partial}{\partial t} \iint_S \left[ \frac{\rho_0 v_n}{r|1 - M_r|} \right]_{\text{ret}} dS \quad (1)$$

$$4\pi p'_L(\mathbf{x}, t) = \frac{1}{c_0} \frac{\partial}{\partial t} \iint_S \left[ \frac{\tilde{p} \cos \theta}{r|1 - M_r|} \right]_{\text{ret}} dS + \iint_S \left[ \frac{\tilde{p} \cos \theta}{r^2|1 - M_r|} \right]_{\text{ret}} dS \quad (2)$$

or, alternatively:

$$\begin{aligned}
4\pi p'_T(\mathbf{x}, t) &= \iint_S \left[ \frac{\rho_0(v_n)}{r|1 - M_r|^2} \right]_{\text{ret}} dS \\
&+ \iint_S \left[ \frac{\rho_0 v_n (r\dot{M}_i \hat{r}_i + c_0 M_r - c_0 M^2)}{r^2 |1 - M_r|^3} \right]_{\text{ret}} dS
\end{aligned} \tag{3}$$

$$\begin{aligned}
4\pi p'_L(\mathbf{x}, t) &= \frac{1}{c_0} \iint_S \left[ \frac{(\tilde{p} \cos \theta + \tilde{p} \dot{n}_i \hat{r}_i)}{r|1 - M_r|^2} \right]_{\text{ret}} dS + \iint_S \left[ \frac{\tilde{p} \cos \theta - \tilde{p} M_n}{r^2 |1 - M_r|^2} \right]_{\text{ret}} dS \\
&+ \frac{1}{c_0} \iint_S \left[ \frac{\tilde{p} \cos \theta}{r^2 |1 - M_r|^3} (r\dot{M}_i \hat{r}_i + c_0 M_r - c_0 M^2) \right]_{\text{ret}} dS
\end{aligned} \tag{4}$$

The resulting acoustic signals are stored into different files, in a suitable form for graphic output. User may also pursue a frequency domain analysis, requiring the determination of a discrete Fourier transform on the acoustic pressure time histories. Since the microphones estimate the *perturbation* signature in the pressure field do not considering the absolute value of pressure in the given point (neglecting possible compensation problems of sensors), the mean value of numerical results is automatically neglected into output files; on the other hand, the action of a 4Hz-filter upon the measured pressure time histories ensures the vanishing of the component at zero frequency. We shall see that this mean value is close to the near field loading noise component: thus it is mostly due to a *lifting* effect, while the far field component directly involves the actual *acoustic* pressure field.

#### 4. Hover test-case

In spite of what is usually observed in rotor acoustic numerical calculations, the hover test-case has not been easy to analyse; this fact simply arises by looking at the experimental data, which often do not meet to respect some simple theoretical expectations. For many observer locations the measured acoustic signatures do not present the expected four pressure peaks and show some very irregular time histories. Furthermore, a hovering rotor should radiate the same noise to observers symmetrically placed with respect to body frame of reference, but the measured signals do not always reflect this condition. These anomalies are more and more evident for observer locations just below the rotor plane ( $-2 \leq x_{mic} \leq 2$ ), so it is possible to think they arise from two main, different reasons. First of all, the presence of a large fuselage probably breaks the signature periodicity, theoretically related to the presence of four equal, *isolated* blades; furthermore, in spite of forward flight condition, where the wake is convected far away from the rotating body, the vorticity is all pushed down just upon the observer locations: thus the acoustic pressure time history measured by microphone array is strongly influenced by a *dirty* aerodynamic field, whose *acoustic influence* is not restricted to blade airload distribution. Probably it would have been useful to place some microphones *in* the rotor plane, to obtain a cleaner measure of acoustic signals as well as just one test-case with a significant thickness noise contribution. Fig. 5 shows the comparison between the measured and predicted acoustic signatures for a hovering rotor at  $M_{tip} = 0.645$ , with an observer location quite far from rotor. The general agreement of two signatures seems good, but numerical prediction is quite far from measured pressure peaks.

No significant improvement has been obtained with an increase of blade panels or a variation of stretching parameters; but the available aerodynamic information has not been completely used, since our pressure distributions have not yet taken into account the presence of transducers along blade leading edge. To include these data into our interpolating model, we exploit the data from isolated transducers

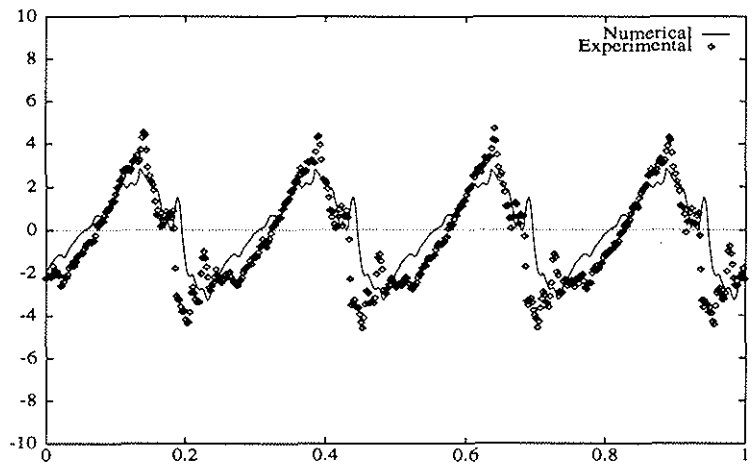


Figure 5 - The agreement between experimental and numerical results is qualitatively quite good, but pressure peaks are not well-predicted. The airload distribution has been here determined with the data-fitting simple model.

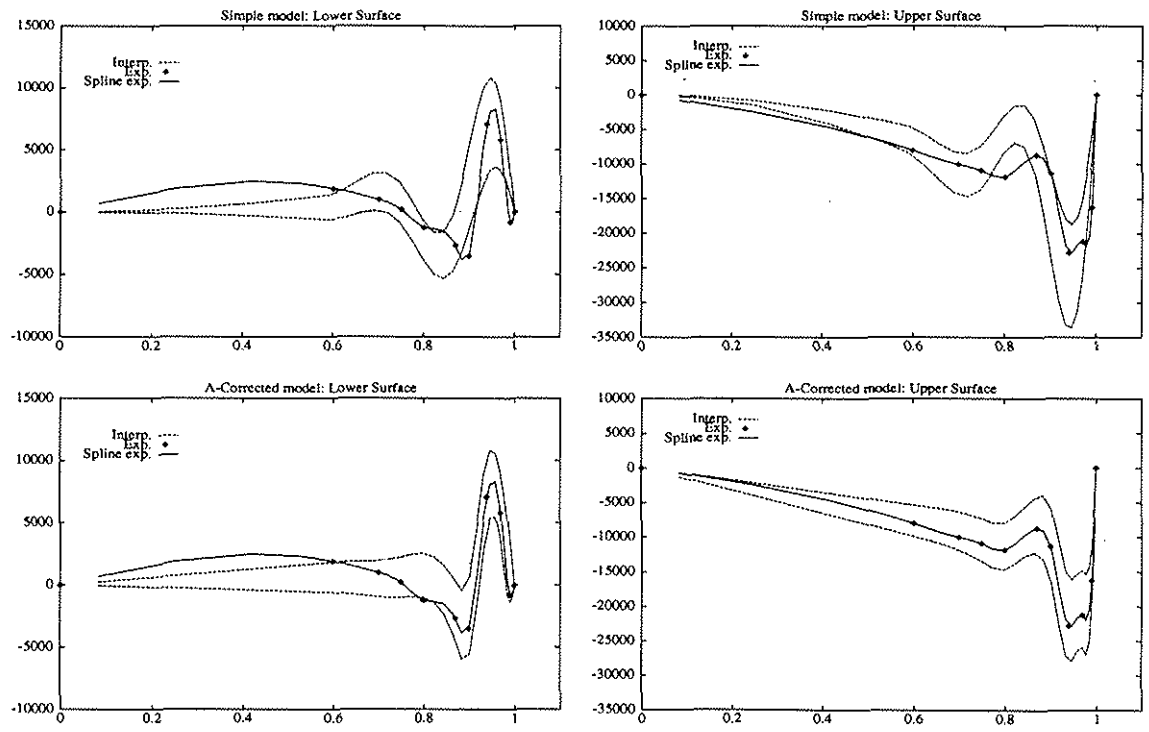
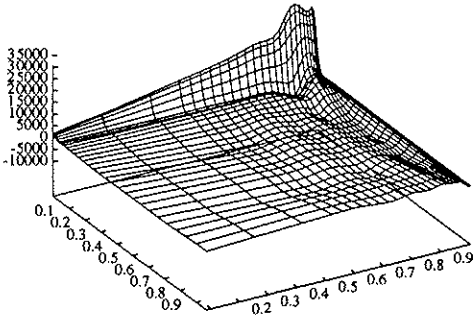


Figure 6 - In this figure the experimental data on fundamental spanwise coordinates are directly interpolated with a cubic-spline; then the curve is compared with the two spanwise pressure distribution, obtained with simple and A-corrected models, referring to the two chordwise coordinates including the X-coordinate of spanwise pressure transducers.

A-Corrected model for data-fitting: pressure on lower surface (Hover test-case)



A-Corrected model for data-fitting: pressure on upper surface (Hover test-case)

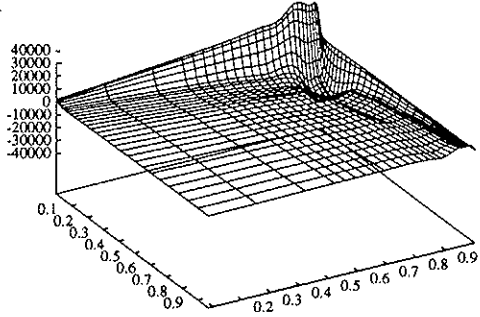


Figure 7 - Blade airload from fitting-data A-corrected model.

to obtain some *additional* fundamental chordwise sections, with a self-similar pressure distribution reconstruction. The calculated cubic spline for fundamental stations is also adopted at spanwise pressure sensor coordinates ( $Y_{transducers} = 0.6, 0.7, 0.8, 0.9, 0.94, 0.99$ ), scaled with the ratio between the single pressure value measured at an isolated transducer and that measured upon the same  $X$ -coordinate of the nearest fundamental chordwise station. We will refer to this interpolating scheme as the *A-corrected* model. Unfortunately the pressure ratio may be very large (especially for lower surface), breaking the regularity of subsequent interpolated airload upon the complete surface; thus a maximum input value is imposed to ensure a *smooth* fitting of aerodynamic data (see section 5). Fig. 6 shows a comparison between the interpolated pressure distributions obtained through simple model and the corresponding A-corrected model, with fixed pressure ratio of 1.5, for the two panel positions nearest to fundamental spanwise coordinates: the A-corrected scheme *captures* the measured values in a better way

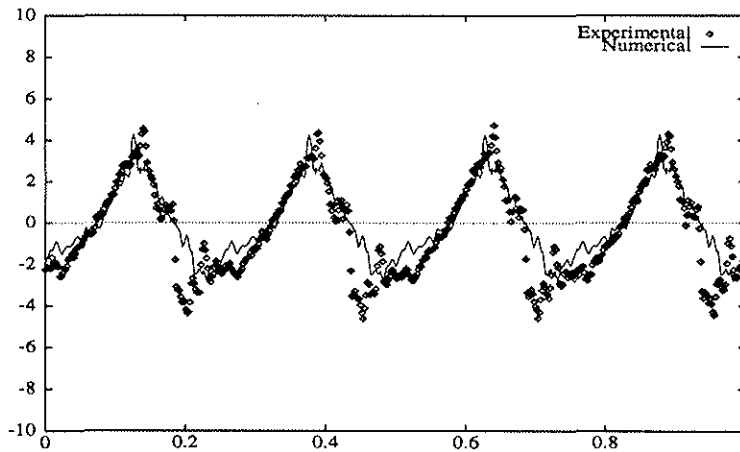


Figure 8 - A remarkable improvement of signatures agreement is obtained through the A-corrected interpolating scheme: the predicted positive peak pressure seems very close to experimental values.

The difference with simple model is more evident, when looking at the three-dimensional views of pressure distribution (Fig. 7). Using the A-corrected model the agreement between experimental and numerical results improves, with a positive pressure peak for predicted signatures very close to measured values (Fig. 8). Note that microphone position  $X_{mic} = -4.0, Y_{mic} = -2.7$  is one of the farthest from rotor: experimental data are very *clean*. Fig. 9 concerns three different test-cases for the hovering rotor. A parabolic stretching has been adopted in numerical grid, for chordwise  $X$ -coordinates near leading edge as well as the outer half blade. Altogether the grid is constituted by 1682 centroids (58 for each airfoil and 29 for each blade spanwise station). The predicted acoustic pressure time histories show a very good agreement with the experimental data.

### 5. Forward flight test-cases

So far no experimental data referring to forward flight conditions were available and the validation of aeroacoustic computational tools for this unsteady aerodynamic problem has always been based on numerical input data. Thus for these cases HELINOISE test-campaign is particularly interesting, especially for high tip speed, where the strong and typical contribution of quadrupole source term is clearly evident inside the measured acoustic signatures. As for the hovering rotor, numerical prediction has begun with the simple data-fitting model, only considering the three fundamental chordwise stations; Fig. 10 shows the comparison for three level flight test-cases: although the experimental data show some irregularity and the measured peak pressures are not the same for every blade, the agreement with computational predictions seems quite satisfactory.

Encouraged by these results, we have tried to improve them with the A-corrected interpolating model, but the numerical signatures has gone through a remarkable worsening! Fig. 11 shows the comparison of two acoustic pressure signatures obtained with simple and A-corrected data-fitting schemes; the latter one has no connection with experimental data neither with the numerical prediction obtained through the simpler interpolating scheme. A explanation of this behaviour may be found in the values of *pressure ratio* calculated for fundamental spanwise pressure transducers. Fig. 12 shows two time histories for measured aerodynamic pressure at  $X = 0.03$  and spanwise locations  $Y = 0.97$  (fundamental station) and  $Y = 0.99$ . In spite of hover condition (where these curves turn into constant values), when the pressure on the nearer fundamental station approaches zero, the ratio with the corresponding value on the isolated sensor strongly increases, and the attempt to build a self-similar airload distribution becomes more and more an arbitrary operation.

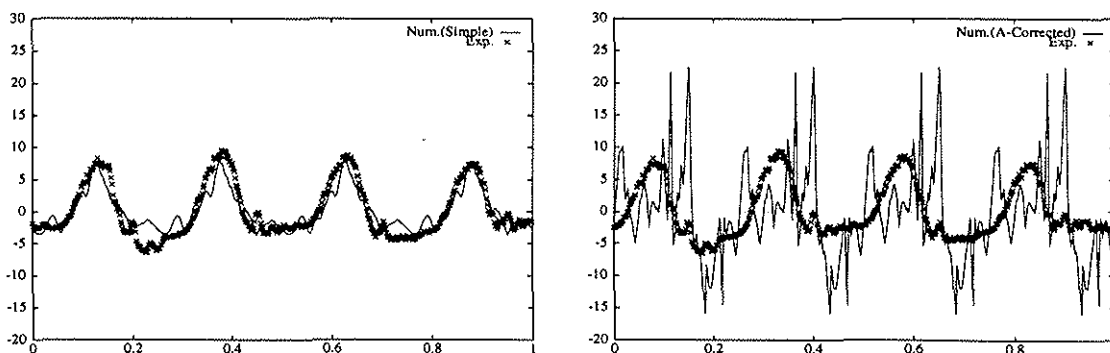


Figure 11 - Comparison of numerical predictions with the two different data-fitting schemes. The A-corrected model result is fully meaningless. This behaviour has been noticed for many microphone locations: probably the figure shows the worst one.

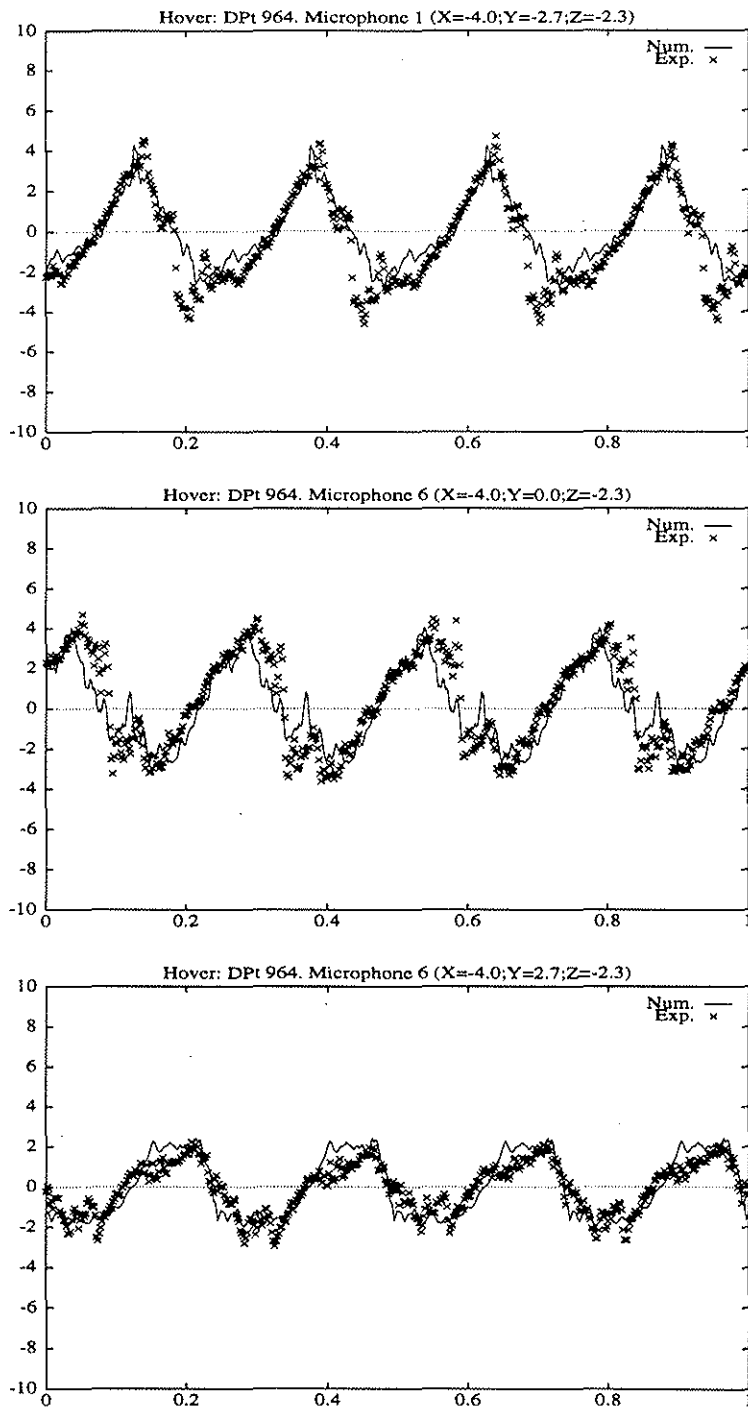


Figure 9 - These three different cases for the hovering rotor have been obtained through the interpolating A-corrected model. The agreement between the two signatures is very satisfactory. The notation DPt964 refers to the test-case number, as reported in [2].

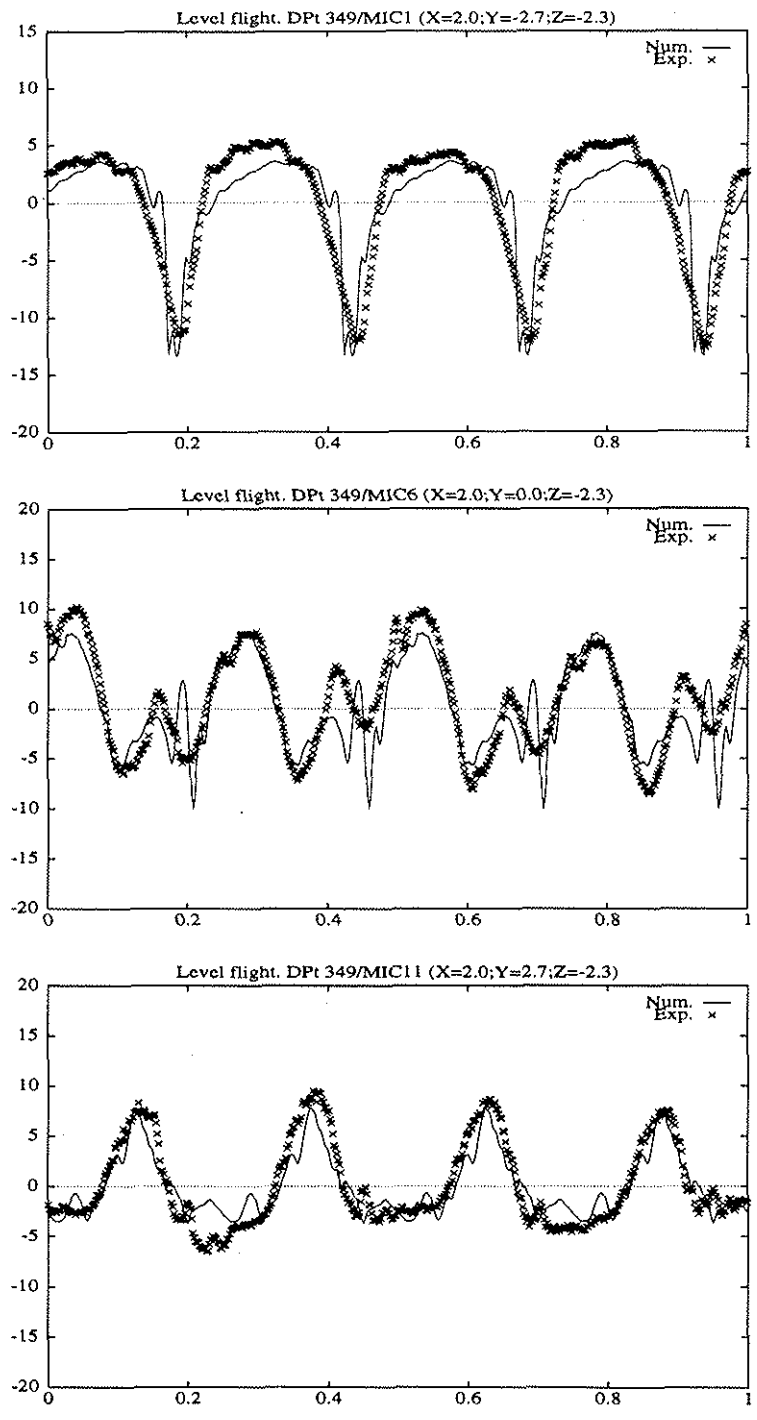


Figure 10 - This results refer to level flight conditions. The airload distributions are determined with the simple data-fitting model and the agreement of numerical prediction with experimental data seems quite good.

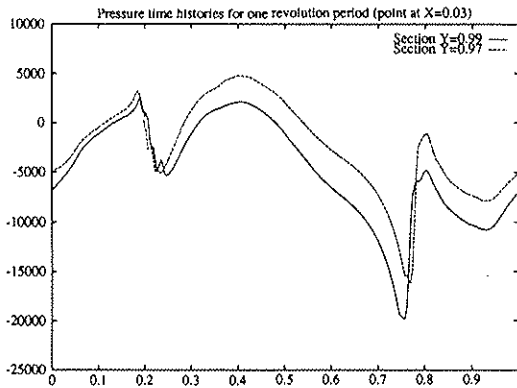


Figure 12 - Pressure time histories measured by two transducers near the blade leading edge ( $X = 0.03$ ) and tip section ( $Y = 0.97$  and  $Y = 0.99$ ). Note that the curves pass through zero for different azimuthal positions.

This condition may appear more than once for each spanwise sensor location; thus, even though a maximum value for pressure ratio is imposed to guarantee a smooth airload distribution, the final result is probably more arbitrary than data-fitting performed by simpler interpolating scheme. Indeed this problem also occurs for the hovering rotor, because for some isolated transducers the measured pressure values are very close to zero; but, since the airload distribution does not change during the revolution period, the imposition of a maximum input value for pressure ratio is sufficient to guarantee a good data-fitting, including the information related to the isolated sensors. On the contrary, the irregular time histories of the pressure for level flight and their frequent sign inversions at different azimuthal positions, make the A-corrected scheme too much sensitive for subsequent acoustic numerical prediction.

Another attempt has been made, in order to exploit the isolated pressure transducers data for blade pressure reconstruction. The additional fundamental chordwise stations were calculated applying a spanwise linear interpolation for the airfoils with the  $Y$ -coordinates of isolated sensors and subsequently imposing the passage of chordwise interpolating cubic spline through the pressure value of the isolated sensor; then the complete spanwise data-fitting was performed as in the other schemes. This approach (named *B-corrected* model) has not given particular improvements with respect to simple model, as it is possible to see in Fig. 13 for two test-cases concerning forward flight conditions.

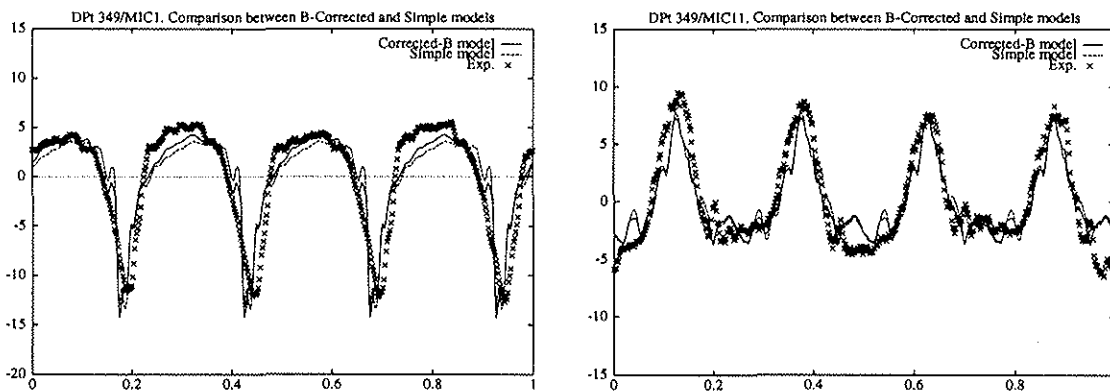


Figure 13 - The attempt to introduce the data from isolated pressure transducers through the B-corrected model has not given particular improvements for the resulting numerical predictions with respect to simple model.

As already mentioned, it is worthwhile to note the single noise contributions, explicitly splitting up the loading noise into far-field and near-field components (Fig. 14). Thickness noise appears quite small and

the shape of the resulting signature is very similar to loading noise far-field component; the near field contribution substantially does not influence the signal shape, only increasing its own mean value. Thus, while the *acoustic* pressure is mainly related to far-field component, the near-field contribution gives a sort of measure of the *aerodynamic* pressure in the field around the blade, related to rotor blades *lifting* effects. The use of a filter at 4Hz in the experimental acoustic measures, cut off this pressure mean value, and the resulting noise signature is very close to the far-field component of loading noise.

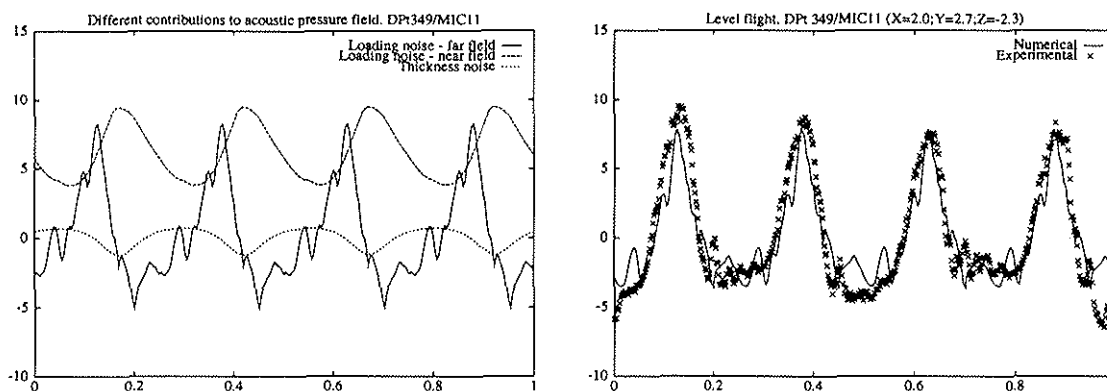


Figure 14 - On the left the different contributions to the acoustic pressure field are shown; note the resemblance of loading noise far-field component with the overall acoustic pressure signature. On the right, the numerical results has been drawn without its own mean value, for the comparison with the experimental signature.

Some other cases have been tested, referring to different flight conditions and using different interpolating schemes; in particular a low speed-12° climb and a low speed-6° descent test-cases are analysed. Note the results for climb flight conditions: even though the data-fitting model only considers the chordwise fundamental stations, the numerical prediction exhibits an excellent agreement with the experimental acoustic pressure signature. On the other hand, this particular test-case shows the cleanest aeroacoustic data, also for microphone locations placed just below the rotor plane ( $X_{mic} = 0.0$ ). Also the aerodynamic pressure time histories, measured by transducers during the revolution period, exhibits a very smooth trend compared with other test-cases, so that the input data are very clean. On the contrary, the descent flight represents a numerical subtle problem, concerning a blade-vortex interaction condition. The simple interpolating model is not able to represent the very complex pressure field, and the available informations are probably insufficient to accurately describe the airload distribution upon the rotating blade: in fact the difference between predicted and measured pressure peaks is more evident just at the position (DPt 1339, MIC11) where BVI is very strong.

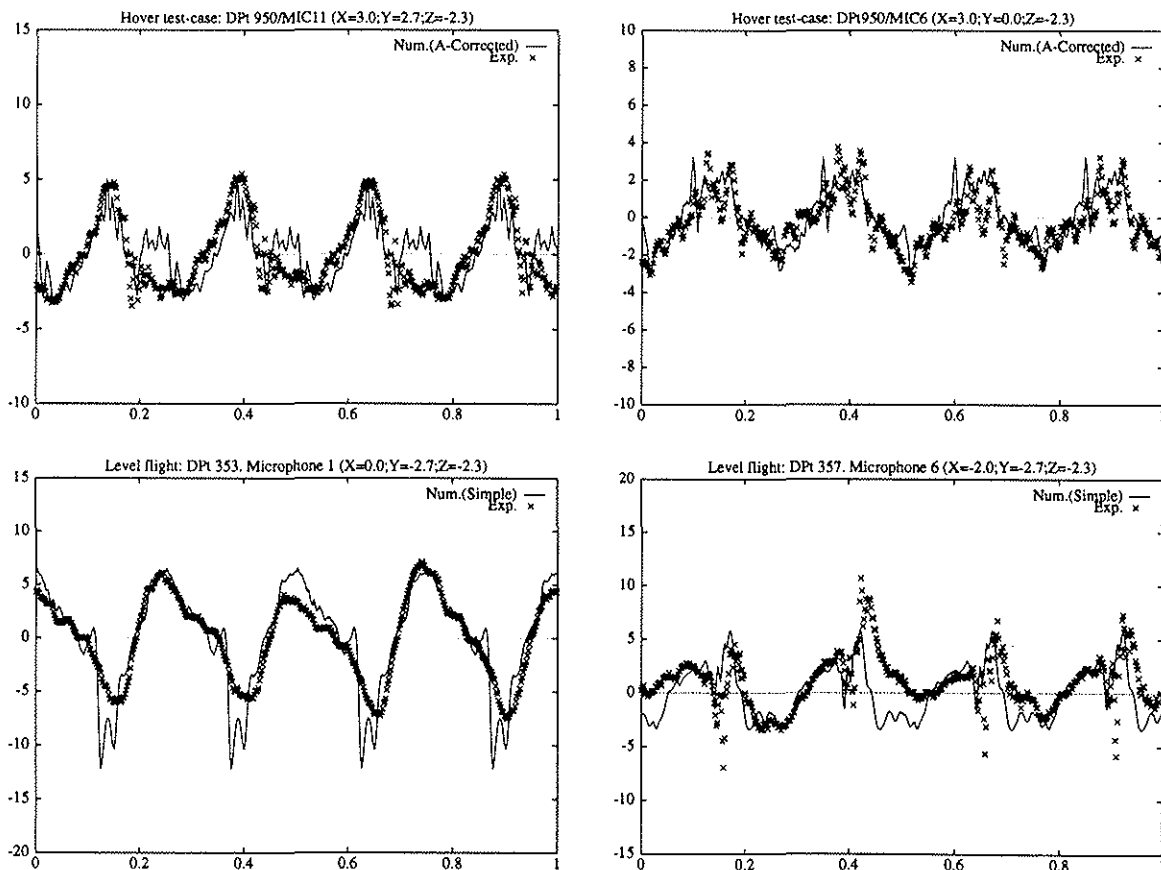
Moreover, all pressure signatures taped by the isolated sensors are very irregular, exhibiting strong oscillations and frequent sign inversions. Thus any attempt to improve numerical prediction through the introduction of spanwise pressure transducers data has produced very instable signatures, whose shape is probably related to numerical problems. Anyhow, there is a marked resemblance between the shape of numerical and experimental result.

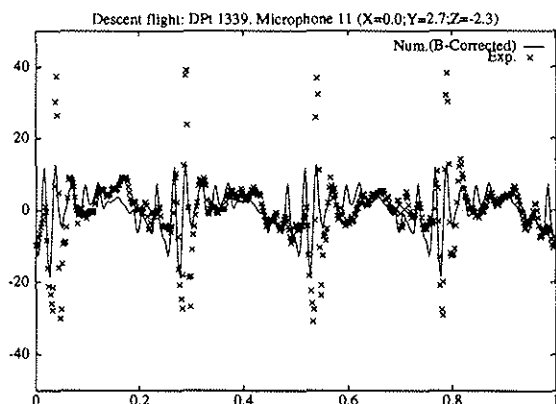
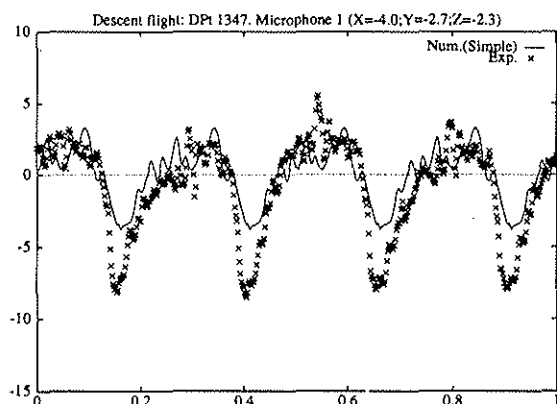
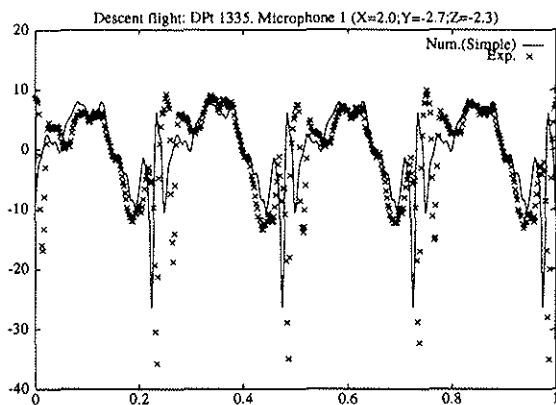
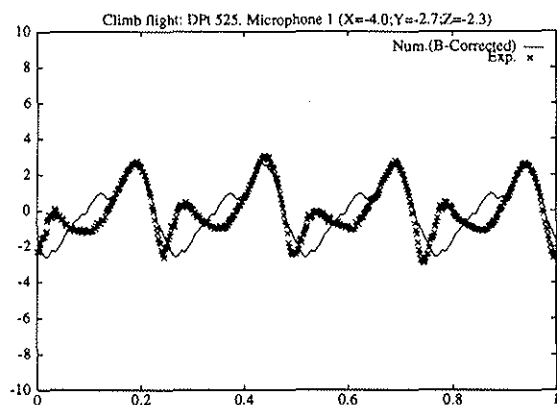
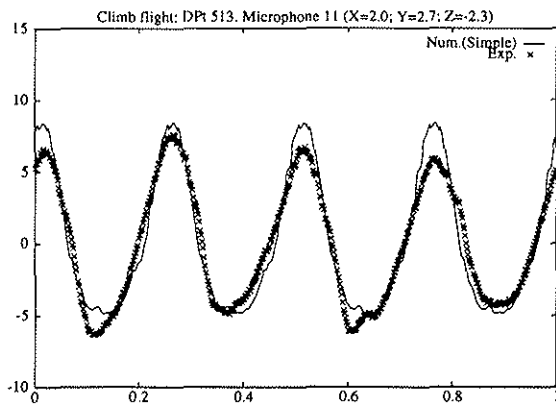
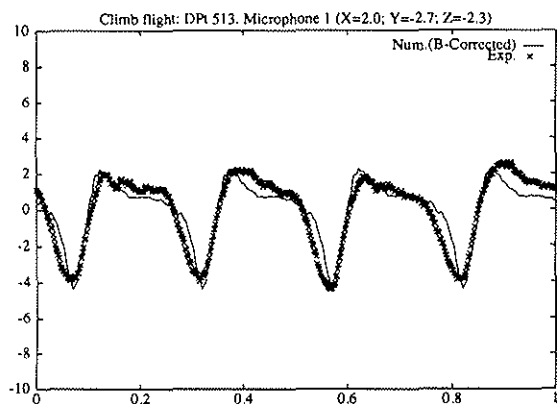
## 6. Conclusions

Several test-cases have been presented comparing numerical prediction to experimental data. Large

data-base obtained during the HELINOISE project has been used; these results have pointed out what kind of problems arise when the pressure values are measured in a wind tunnel and exploited for numerical calculations. No particular data-fitting model may be considered the *best*; rather it has to be adapted to the single test-case one has to treat: it does not always happen that a more complex interpolating scheme provides better numerical predictions. The presence of isolated pressure transducers along blade leading edge provides an important knowledge for blade airload reconstruction; nevertheless this information is very difficult to exploit. From a computational point of view, it would be more useful to place some other transducers chordwise to numerically determine a more accurate pressure distribution. Many other data-fitting models may be applied, of course; for example it is possible to consider directly a two-dimensional scheme based on spline surface, or a least-square approach, abandoning the condition for interpolating model to pass through the experimental points.

Anyhow this paper proves the reliability of present numerical procedures in the prediction of rotor noise signatures and, above all, the excellent quality of experimental data, both aerodynamic and acoustic, measured in DNW wind tunnel. This quality becomes crucial for other test-cases concerning high tip speed blades, in view of the development and validation of new computational techniques for the prediction of quadrupole source term contribution to the acoustic pressure field.





## References

- 1 S. IANNIELLO, M. GENNARETTI, G. GUJ, E. DE BERNARDIS, Validation of a New Code for the Prediction of Noise Generated by Helicopter Rotor, *paper presented at 19th European Rotorcraft Forum, Paper No. B6*, Cernobbio - Villa Erba, Italy, 14-16 September 1993.
- 2 W. R. SPLETTSTOESSER, B. JUNKER, K. J. SCHULTZ, W. WAGNER, W. WEITEMEIER, A. PROTOPSALTIS, D. FERTIS, The HELINOISE Aeroacoustic Rotor Test in the DNW - Test Documentation and Representative Results, *DLR-Mitt. 93-09*, Braunschweig, December 1993.